The Potential Energy Surfaces of Ga-HCN

V.J.F. Lapoutre

November 2, 2008

Contents

Chapter 1

Introduction

In recent years, the importance of van der Waals complexes in the entrance channel has been more and more recognized.[1,2] To understand these complexes, measurements[3] and calculations[1,2,4,5] have been done. The calculation of the bound state of a closed shell system via the potential energy surface (PES) is well understood by now. Using the Born-Oppenheimer approximation, first the potential energy surface of the ground state is calculated. Using this PES and neglecting the non-adiabatic couplings the bound state can be determined. However, the same kind of calculation for an open shell system is much more challenging, because more than one state is involved. This gives both problems with the non-adiabatic couplings and with the counterpoise correction (see also chapter 2).

This project is about the interaction between gallium and HCN. It is interesting to calculate the bound states of this system, because they can be compared to experimental results.[6] To calculate these bound states, we start with *ab initio* calculations of the potential energy surfaces.

Chapter 2

Open-shell Complexes

In a complex with an open-shell atom where the unpaired electron can be in one of several states, there exists more than one adiabatic potential energy surface. In gallium, there is only one electron in the 4p shell, so this one can be in either the p_x, p_y or p_z orbital. In the interaction with the linear molecule HCN, every occupation has a different interaction with the HCN molecule. In the linear orientation of gallium with HCN, the two Π states are degenerate due to symmetry reasons. This leads to the breakdown of the Born-Oppenheimer approximation, commonly used in quantum chemistry.

The time-independent Schrödinger equation is usually formulated as

$$\hat{H}\Psi = E\Psi, \tag{2.1}$$

where $\hat{H}$ is the relevant Hamiltonian for the problem. Ψ is then an eigenfunction of the Hamiltonian and describes the state of the system and E is the energy of the system. Ψ can be written for the nuclei and the electrons seperately as follows $\sum_{j=1}^{\infty} \chi_j(\boldsymbol{Q})\phi_j(\boldsymbol{q},\boldsymbol{Q})$. $\boldsymbol{Q}$ describes the nuclear positions and $\boldsymbol{q}$ these of the electrons. The $\phi_j(\boldsymbol{q},\boldsymbol{Q})$ are the eigenfunctions of the electronic Hamiltonian for fixed $\boldsymbol{Q}$:

$$\hat{H}_{el}(\boldsymbol{q},\boldsymbol{Q})\phi_j(\boldsymbol{q},\boldsymbol{Q}) = V_j(\boldsymbol{Q})\phi_j(\boldsymbol{q},\boldsymbol{Q}) \tag{2.2}$$

This equation can be also formulated as[7, 8]

$$\left(-\frac{\nabla^2_{\boldsymbol{Q}}}{2M} + V_j(\boldsymbol{Q}) - E\right)\chi_j(\boldsymbol{Q}) = \sum_{k=1}^{\infty}\left(\boldsymbol{F}_{jk}\cdot\boldsymbol{\nabla}_{\boldsymbol{Q}} + \frac{1}{2}G_{jk}\right)\chi_k(\boldsymbol{Q}), \tag{2.3}$$

with coupling coefficients

$$\boldsymbol{F}_{jk}(\boldsymbol{Q}) = \frac{1}{M}\langle\phi_j(\boldsymbol{q},\boldsymbol{Q}) \mid \boldsymbol{\nabla}_{\boldsymbol{Q}}\phi_k(\boldsymbol{q},\boldsymbol{Q})\rangle, \tag{2.4}$$

$$G_{jk}(\boldsymbol{Q}) = \frac{1}{M}\langle\phi_j(\boldsymbol{q},\boldsymbol{Q}) \mid \nabla^2_{\boldsymbol{Q}}\phi_k(\boldsymbol{q},\boldsymbol{Q})\rangle. \tag{2.5}$$

Here, M represents the nuclear masses and $V_j(\boldsymbol{Q})$ the potential energy surface for fixed nuclear orientation. The off-diagonal elements of these couplings are called the non-adiabatic couplings.

In the Born-Oppenheimer approximation, the right part of equation 2.3 is neglected. Usually this is appropriate, since the coupling coefficients are very small due to the large M. However, when two or more states are degenerate these coupling coefficients become very large. This can be seen more clearly when reformulating the expression as follows[7]:

$$\boldsymbol{F}_{jk}(\boldsymbol{Q}) = \frac{1}{M} \frac{\langle \phi_j(\boldsymbol{q}, \boldsymbol{Q}) \mid \boldsymbol{\nabla}_{\boldsymbol{Q}} H_{el} \mid \phi_k(\boldsymbol{q}, \boldsymbol{Q}) \rangle}{V_k(\boldsymbol{Q}) - V_j(\boldsymbol{Q})} \tag{2.6}$$

The expression for $G_{jk}(\boldsymbol{Q})$ can be rewritten in a similar way.

The calculations done to obtain a potential energy surface, give the adiabatic states. These states $\phi_j(\boldsymbol{q}, \boldsymbol{Q})$ are eigenfunctions of the electronic Hamiltonian $\hat{H}_{el}$. For a closed-shell system, this potential energy surface (PES) is the end-point of the first step of the Born-Oppenheimer approximation. However, for an open-shell system, it is not so easy, as shown above. A possibility to solve this problem is calculate other states which strongly reduce the non-adiabatic couplings[9]. These states are called the diabatic states and they are a linear combination of the adiabatic states, in such a way that the kinetic energy coupling is minimal. How to get these, will be explained in chapter 4.

Chapter 3

Adiabatic Potential Energy Surfaces

The system was oriented in the xz-planee, with the gallium atom in the origin. The vector between the center-of-mass of HCN and gallium is the z-axis. The relevant Jacobi coordinates are shown in Fig. 3.1

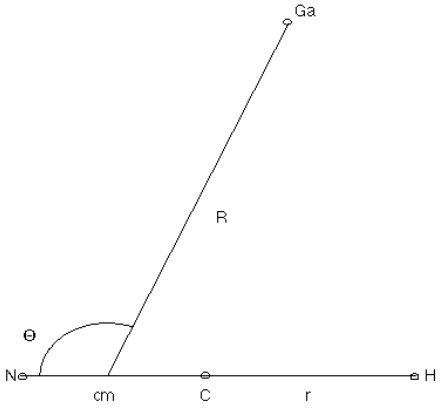

Figure 3.1: The Ga-HCN system and its relevant Jacobi coordinates R, r and θ (arbitrary values for these coordinates were chosen in this picture)

Gallium is in the fourth row of the periodic table and has the electron configuration $[Ar]4s^2 3d^{10} 4p^1$. Due to the unpaired electron in the 4p orbital, the system is open shell. HCN is always regarded as being linear, we varied only the C-H distance. [10]

The energies were computed on a 14 × 12 × 5-dimensional grid. The following 14 R values were included: $R = 4.5$, 5.0, 5.5, 6.0, 6.5, 7.0, 7.5, 8.0, 9.0, 10.0, 12.5, 15.0, 20.0 and 25.0 a_0. The θ-grid was a 12 point Gauss-Legendre grid, and the same five C-H distances were taken as in the paper of Fishchuk et al. [10], they are 1.666, 1.855, 2.044, 2.233 and 2.422 a_0. The third one, 2.044

a_0, is the equilibrium distance and will be calles r_e.

The energy calculations were performed using the RCCSD(T) method [11] for open shell systems. All calculations were done using the MOLPRO package [12]. The atomic orbital basis set used was the augmented correlation-consistent polarized triple-ζ basis (aug-cc-pVTZ) with uncontracted bond functions (exponents sp = 0.9, 0.3, 0.1 and d = 0.6, 0.2) added halfway between the gallium and the nearest atom of the HCN molecule. The active space in the CASSCF calculations contains the relevant $4p$ orbitals. In the RCCSD(T) calculations, the valence orbitals of H, C and N and the 4s and 4p orbitals from gallium were used for the excitations.

The complex of gallium and linear HCN has C_s symmetry. It possesses three potential energy surfaces corresponding to the ^{2}P ground state of the free Ga atom. Two of these three potential energy surfaces have A' symmetry, they correspond to the unpaired electron occupying one of the $4p_x$ and $4p_z$ orbitals of the gallium atom. The state with A" symmetry has a singly occupied $4p_y$ orbital in the gallium atom. We can compute the ground state for each symmetry, this is $\Psi_1(A')$ for the A' symmetry and $\Psi(A")$ for the A" symmetry. However, the second state with A' symmetry, $\Psi_2(A')$ is not a ground state and it is therefore not straightforward how to compute the energies for this state using the RCCSD(T) method. To force MOLPRO to calculate this state, a trick had to be used. When looking at the different MO's, the singly occupied orbital in the A" symmmetry is always the $4p_y$ orbital, where the singly occupied orbital in the A' symmetry is in general a linear combination of the $4p_x$ and $4p_z$ orbitals. This can also be expressed as a rotation of these orbitals in the following way:

$$(\varphi_1(A'), \varphi_2(A')) = (4p_x, 4p_z) \begin{pmatrix} \cos\gamma_{orb} & \sin\gamma_{orb} \\ -\sin\gamma_{orb} & \cos\gamma_{orb} \end{pmatrix}. \tag{3.1}$$

At small angles θ the orbital $\varphi_1(A')$ is almost fully $4p_x$, so γ_{orb} is (very) close to zero. However, when θ is large, $\varphi_1(A')$ is almost fully $4p_z$. To calculate $\Psi_2(A')$ we want to swap the two orbitals with the $4p$ character, this can be done by the rotate keyword in MOLPRO. For the calculations on the complex, these are numbers 17.1 and 18.1, for the gallium fragment these are orbitals number 12.1 and 13.1. [1]

In Fig. 3.2 the molecular orbitals are given and it is shown whether they consist mainly of Ga atomic orbitals or HCN atomic orbitals. Only molecular orbitals consisting of valence atomic orbitals are considered. The gallium orbitals are from low to high: $3d$, $4s$ and $4p_y$. For HCN it is more difficult, since also in the monomer the molecular orbitals are mixtures of many atomic orbitals. The lowest HCN-orbital consists mainly of the $2s$ orbitals of C and N, the second lowest contains the $1s$ orbital of H and the $2p_x$ and $2s$ orbitals of C. The highest three orbitals are combinations of the $2p_x$, $2p_y$ or $2p_z$ orbitals of carbon and nitrogen, where the combination of the p-orbitals in the molecular axis (σ) is lower in energy.

When correcting for the bsse as in Fishchuk et al. [1], namely getting the interaction energy by subtracting from the energy of the complex the HCN energy and the *lowest* Ga energy (both calculated in orbital basis set of the full complex), we encountered a problem with the energies of the Ga. At the start of the calculation, MOLPRO calculates first the lowest gallium energy and after the orbital-swap it calculates an energy which is (slightly) higher. However,

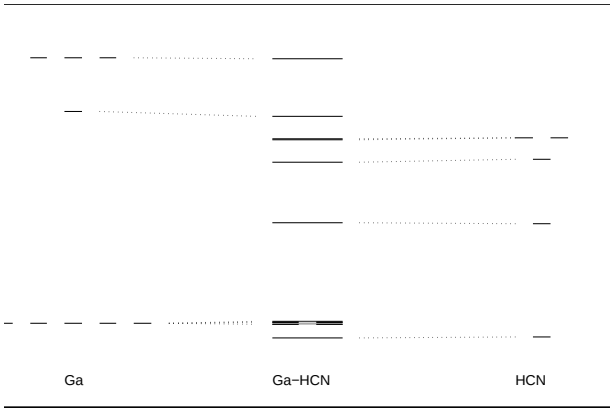

Figure 3.2: An MO-diagram of the A" state with $R = 7.5$, $r_{HC} = r_e$ and $\theta = 82.8$. The highest Ga-HCN orbital is singly occupied, because only one of the highest gallium orbitals is singly occupied. All HCN orbitals are doubly occupied.

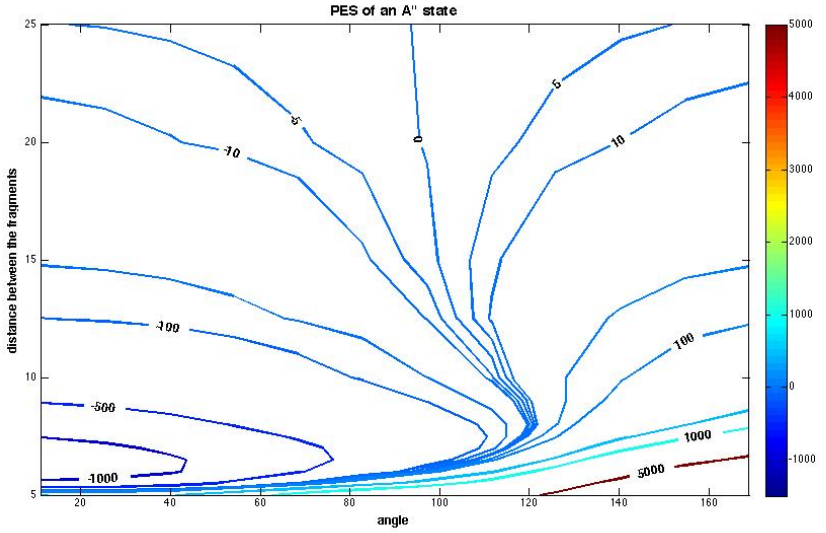

Figure 3.3: The adiabatic potential energy surface for the A" state.

from some point, it calculates first the higher energy and after the swap gives a lower energy, both for the coupled cluster as for the HF results. This might be because the calculation of the HF orbitals starts from the result of the previous calculation. Therefore, the unswapped orbital results are probably very similar as are the swapped results.

For some of the grid points we didn't obtain all the RCCSD(T) energies we need. Sometimes, this was because the iterations did not converge. Other times, we would get a normal RCCSD(T) energy for the $\Psi_1(A')$ state, but performing the orbital swap did not work. Before the RCCSD(T) calculation, we also did a RHF calculation on the swapped system and sometimes this gave immediately the unswapped state. A third problem we encountered arose because of the ordering of the orbitals. In the RCCSD(T) calculations of the monomers, the valence orbitals of the atoms were used for the excitations. In the complex, we want to use more or less the same orbitals for the excitations, so also the molecular orbitals which are the linear combinations of the valence orbitals of the atoms as active space. Sometimes, the ordering would be such, that the energies of the first orbitals of the valence atoms were close to the energies of the other orbitals, and this might give a "wrong" ordering, i.e. an ordering which didn't give a sensible interaction energy. This problem was easily solved by swapping the orbitals so the valence orbitals are the highest occupied orbitals and these are used for the excitations.

The potential energy surfaces for the three adiabatic states with $r_{HC} = r_e$ are given in Fig. 3.3 to Fig. 3.5.

In Fig. 3.6 the three different adiabatic states are shown, where $R = 7.0$ and $r_{HC} = r_e$. At $\theta = 0$ and $\theta = \pi$, the A" state should be degenerate with one of the A' states. In the figure it is shown that close to the linear orientations, the orbitals are also nearly degenerate. In Fig. 3.7, $R = 25$. Also here, the A" state is almost degenerate with one of the A' orbitals close to the linear orientations,

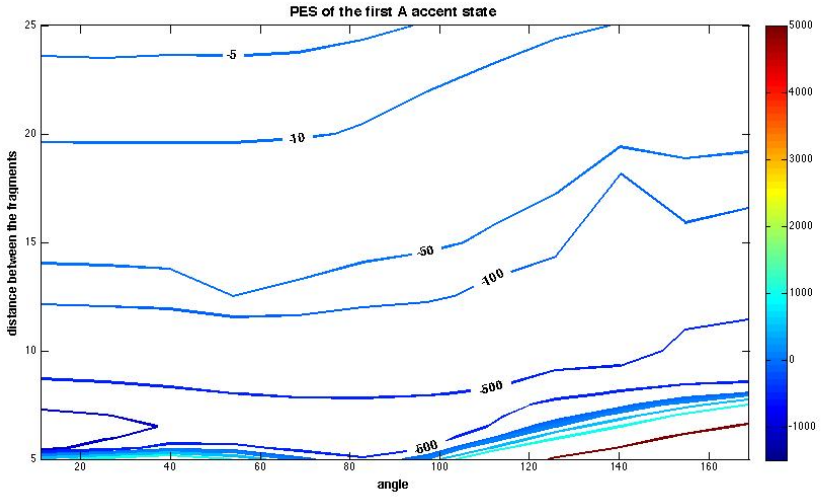

Figure 3.4: The adiabatic potential energy surface for the 1A' state.

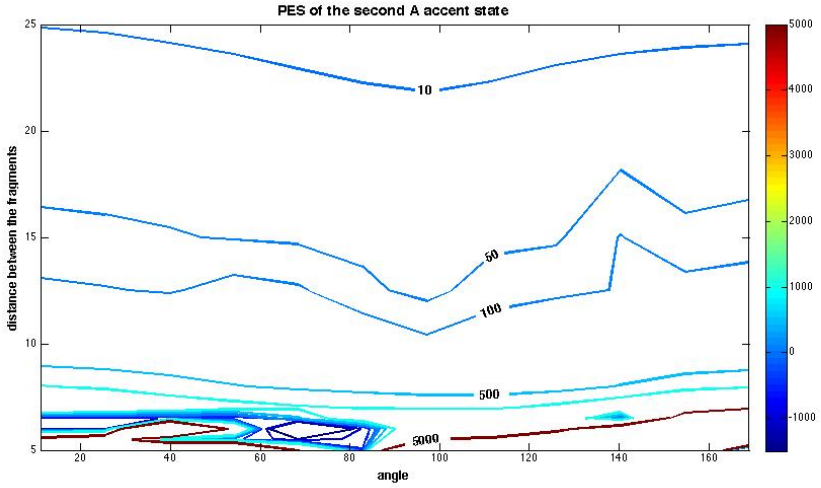

Figure 3.5: The adiabatic potential energy surface for the 2A' state.

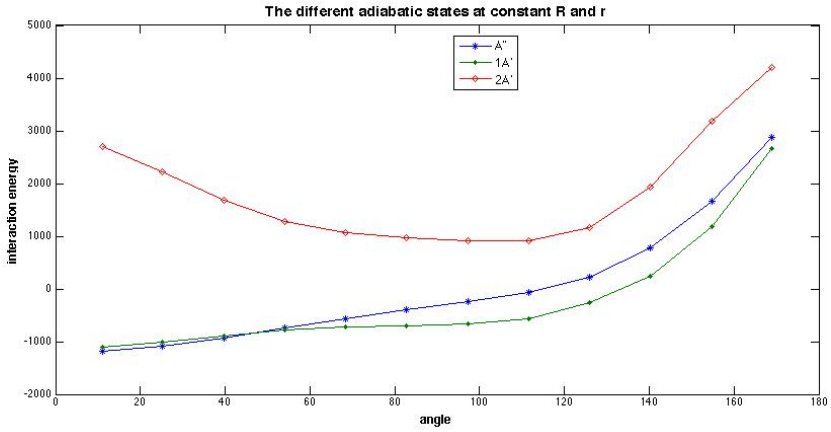

Figure 3.6: The three adiabatic states with R=7.

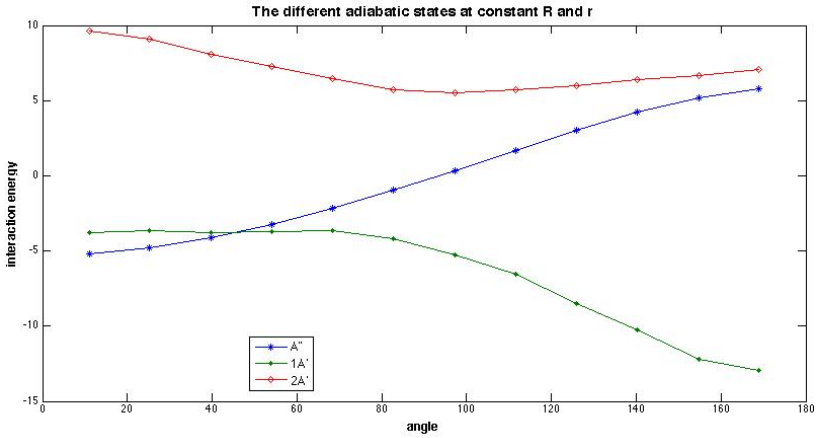

Figure 3.7: The three adiabatic states with R=25.

but close to $\theta = \pi$, it is degenerate with the $\Psi_2(A')$ state where at shorter R, it is close to degenerate with the $\Psi_1(A')$ state. However, the states are almost degenerate. In a plot of the uncorrected energy (Fig. 3.8) it can be seen that there the states are much more degenerate.

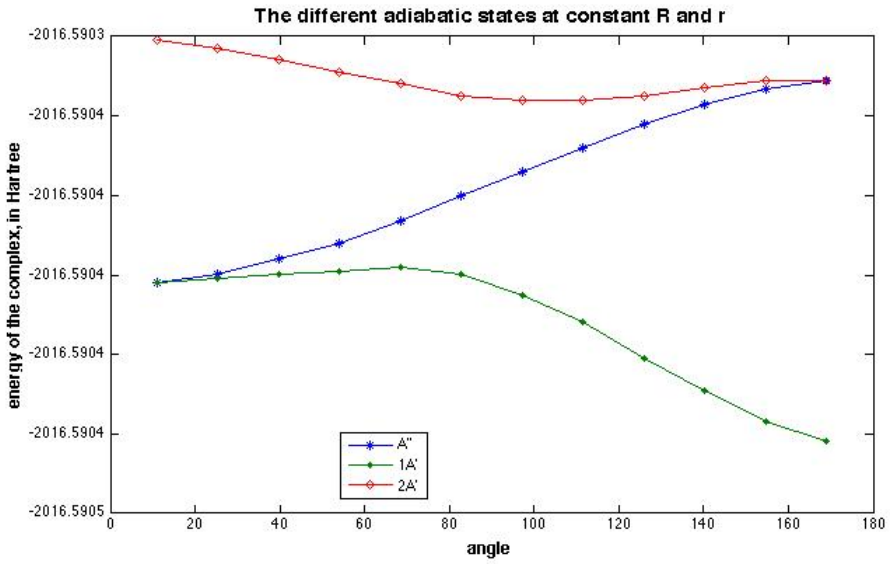

Figure 3.8: The energy of the Ga-HCN of the three adiabatic states with R=25. No counterpoise correction was done.

Chapter 4

Diabatic Potential Energy Surfaces

Now the adiabatic potential energy surfaces are known, we can not yet solve the nuclear motion problem. The non-adiabatic couplings are much too large to be able to neglect them as is done in the Born-Oppenheimer approximation (see chapter 2). We need to go to a basis where the non-adiabatic couplings become small.

This basis is the diabatic basis. We can obtain this basis by a rotation of the adiabatic states over an angle γ in the following way:

$$(\Psi_1(A'), \Psi(A"), \Psi_2(A')) = (\mid P_x\rangle, \mid P_y\rangle, \mid P_z\rangle)\, \mathbb{R}_y(\gamma) \tag{4.1}$$

where

$$\mathbb{R}_y(\gamma) = \begin{pmatrix} \cos\gamma & 0 & \sin\gamma \\ 0 & 1 & 0 \\ -\sin\gamma & 0 & \cos\gamma \end{pmatrix} \tag{4.2}$$

This angle indicates how the p_x and p_z states are rotated around the y-axis, or how much they are mixed to form the adiabatic states. The angle γ is therefore also called the mixing angle.[2, 1, 13, 9] The mixing angle was calculated by

$$\gamma = \arctan\left[\frac{\langle\Psi(A'') \mid L_z \mid \Psi_2(A')\rangle}{\langle\Psi(A'') \mid L_z \mid \Psi_1(A')\rangle}\right] \tag{4.3}$$

where L_z is the the z-component of the gallium electronic angular momentum operator. These matrix elements were obtained using CASSCF and MRCI calculations.[14, 15] The values for γ form a smooth surface, where the absolute value at large R goes from zero at $\theta = 0$ to $\frac{\pi}{2}$ at $\theta = \pi$. For small R, this is completely different and also at θ close to 180 degrees, the value for γ is small. However, at the points calculated with $\theta = 82.8$, the CASSCF calculations of $\Pi_2(A')$ are often wrong, which is visible from the very high energy of these states. Because of these wrong states, also the MRCI states and matrix elements at these points are wrong, see also Fig. 4.1. So, neither could the mixing angle be calculated well. To obtain the right results, these points have to be properly fitted.

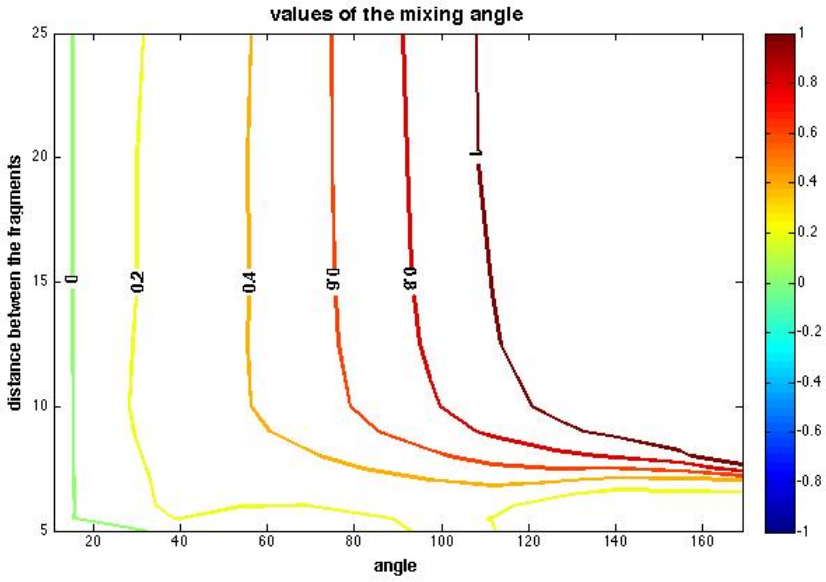

Figure 4.1: The values for the mixing angle γ at r_e.

When the basis is transformed, the potential energy surfaces relate to the adiabatic potential energy surfaces in the following way

$$\begin{aligned} V_{xx} &= V_1(A')\cos^2\gamma + V_2(A')\sin^2\gamma \\ V_{zz} &= V_1(A')\sin^2\gamma + V_2(A')\cos^2\gamma \\ V_{xz} &= [V_2(A') - V_1(A')]\sin\gamma\cos\gamma \\ V_{yy} &= V(A'') \end{aligned} \tag{4.4}$$

If we go to a spherical basis, there are only small non-adiabatic couplings between the different states anymore.[9] The transformation to this basis is as follows for the states

$$(\mid P_x\rangle, \mid P_y\rangle, \mid P_z\rangle) = \frac{1}{\sqrt{2}}(\mid P_{-1}\rangle, \mid P_0\rangle, \mid P_1\rangle) \begin{pmatrix} 1 & \imath & 0 \\ 0 & 0 & \sqrt{2} \\ -1 & \imath & 0 \end{pmatrix} \tag{4.5}$$

and for the potential energy surfaces[1]

$$\begin{aligned} V_{0,0} &= V_{zz} \\ V_{1,1} = V_{-1,-1} &= \tfrac{1}{2}(V_{yy} + V_{xx}) \\ V_{1,-1} &= \tfrac{1}{2}(V_{yy} - V_{xx}) \\ V_{0,1} = -V_{0,-1} &= -\tfrac{\sqrt{2}}{2}V_{xz} \end{aligned} \tag{4.6}$$

Fig. 4.2 to Fig. 4.5 show some of these diabatic potential energy surfaces. The results near $\theta = 80$ are not accurate due to the problems with the mixing angle.

These are the diabatic potential energy surfaces which can be conveniently used to solve the nuclear motion problem. The non-adiabatic couplings are now replaced in a coupling via the different potential energy surfaces.

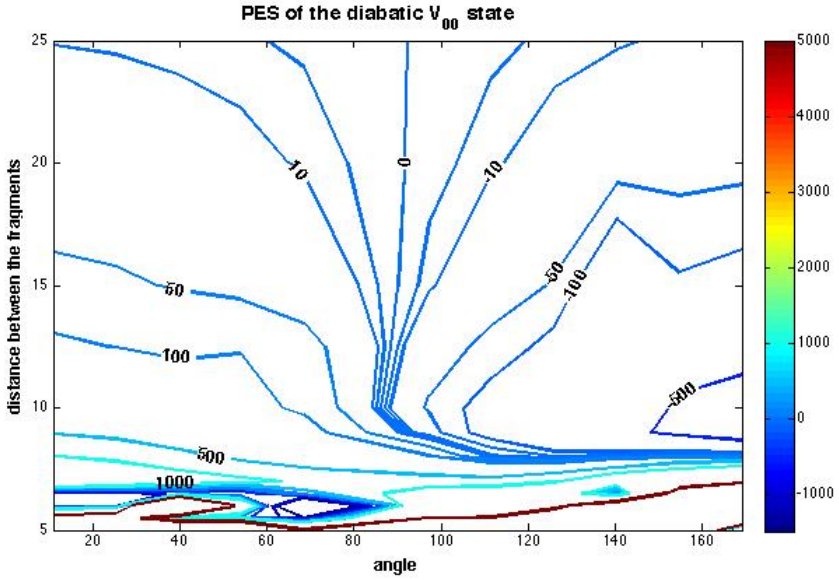

Figure 4.2: The diabatic potential energy surface $V_{0,0}$.

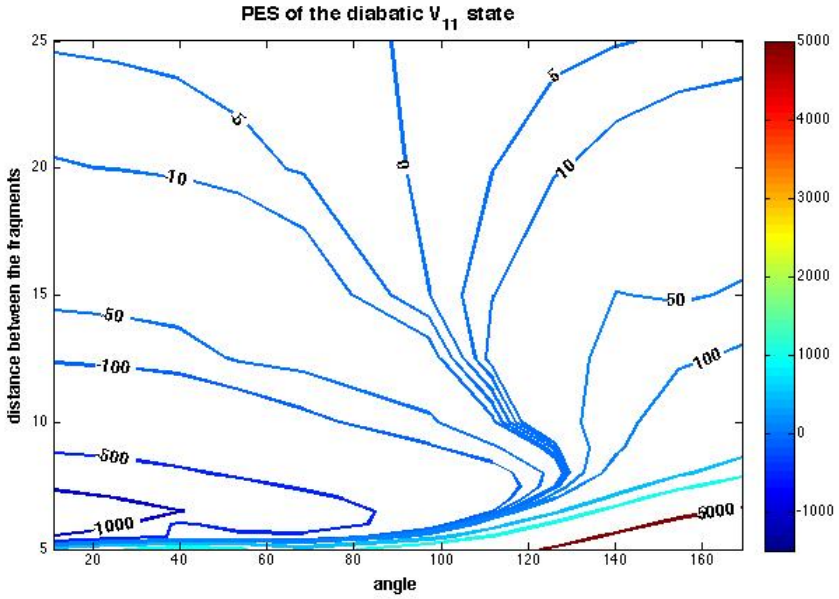

Figure 4.3: The diabatic potential energy surface $V_{1,1}$.

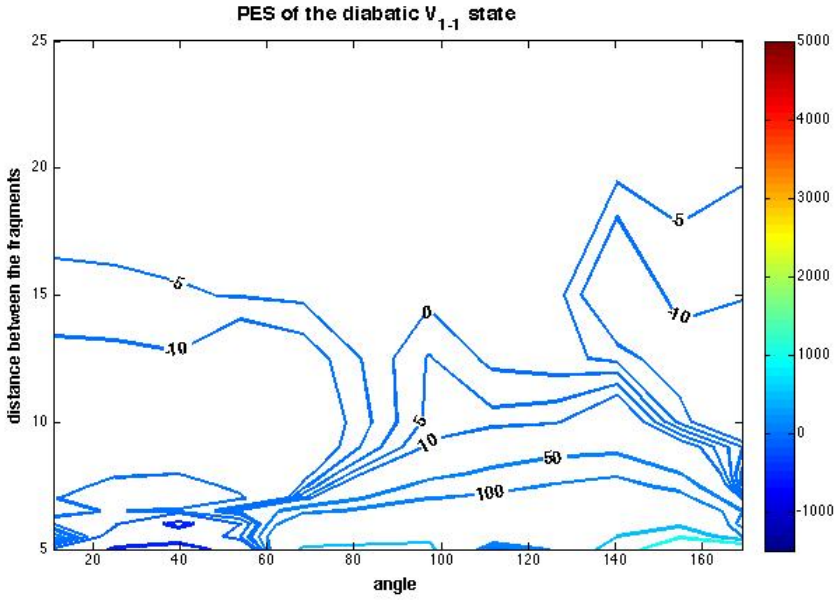

Figure 4.4: The diabatic potential energy surface $V_{1,-1}$.

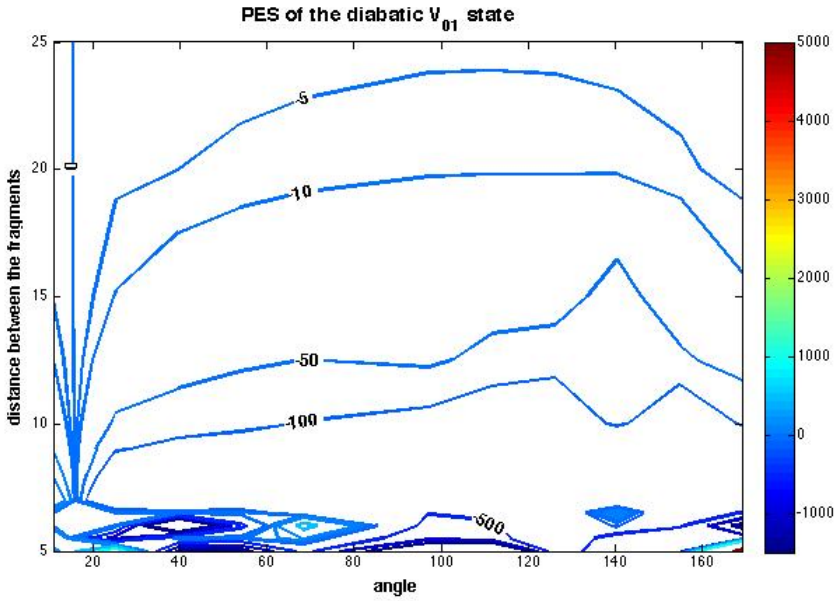

Figure 4.5: The diabatic potential energy surface $V_{0,1}$.

Chapter 5

Conclusion

The numerical values for the energy on the grid mentioned in chapter 3 are known. Some points have to be interpolated because the CC calculation did not converge. This is mainly the problem with short R and R values around 12.5 a_0. All the points should be fitted to give the potential energy surfaces $V_1(A')$, $V(A")$ and $V_2(A')$. When these are known, the method from chapter 4 together with the results from the MRCI calculations can be used to construct the diabatic potential energy surfaces $V_{0,0}$, $V_{1,1}$, $V_{-1,-1}$, $V_{1,-1}$, $V_{0,1}$ and $V_{0,-1}$. In these potential energy surfaces and the respective states, the non-adiabatic couplings are replaced by couplings between the potential energy surfaces. This gives that these potential energy surfaces can be used to calculate the bound states of the complex and compare these theoretical results with the experiments.

The bsse, estimated by comparing the gallium and HCN energies calculated in the basis of the complex and both calculated on their own, is in the order of the interaction energy. It gets smaller as the fragments are further away from each other, but is still significant.

Bibliography

[1] A. V. Fishchuk, P. E. S. Wormer, and A. van der Avoird. Ab initio treatment of the chemical reaction precursor complex Cl(^{2}P)-HF. 1. three-dimensional diabatic potential energy surfaces. *J. Phys. Chem. A*, 110: 5273, 2006.

[2] M. H. Alexander. Adiabatic and approximate diabatic potential energy surfaces for the B$\cdots$ H $_2$ van der waals molecule. *J. Chem. Phys.*, 99(8): 6014, 1993.

[3] K. Hinds and A. C. Legon. The geometry and intermolecular binding of HCN ... BrCl probed by rotational spectroscopy. *Chem. Phys. Lett.*, 240: 467, 1995.

[4] A. van der Avoird, T. B. Pedersen, G. S. F. Dhont, B. Fernández, and H. Koch. *Ab initio* potential-energy surface and rovibrational states of the HCN-HCl complex. *J. Chem. Phys.*, 124:204315, 2006.

[5] B. Bussery-Honvault, J.-M. Launay, T. Korona, and R. Moszynski. Theoretical spectroscopy of the calcium dimer in the $A\ ^1\Sigma_u^+$, $c\ ^3\Pi_u$, and $a\ ^3\Sigma_u^+$ manifolds: An *ab initio* nonadiabatic treatment. *J. Chem. Phys.*, 125: 114315, 2006.

[6] J. M. Merritt, G. E. Douberly, P. L. Stiles, and R. E. Miller. Infrared spectroscopy of prereactive aluminium-, gallium-, and indium- HCN entrance channel complexes solvated in helium nanodroplets. *J. Phys. Chem. A*, 111 (49):12304, 2007.

[7] W. P. J. B. Zeimen. *Dynamics of open-shell van der Waals complexes.* PhD thesis, University of Nijmegen, 2004.

[8] H. Köppel, L. S. Cederbaum, and W. Domcke. Interplay of Jahn-Teller and pseudo-Jahn-Teller vibronic dynamics in the benzene cation. *J. Chem. Phys.*, 89(4):2023, 1988.

[9] V. J. F. Lapoutre. Literature thesis: Potential energy surface calculations of open-shell systems, 2008.

[10] A. V. Fishchuk, J. M. Merritt, and A. van der Avoird. Ab initio treatment of the chemical reaction precursor complex Br(^{2}P)-HCN. 1. adiabatic and diabatic potential surfaces. *J. Phys. Chem. A*, 111(31):7262, 2007.

[11] P. J. Knowles, C. Hampel, and H.J. Werner. Coupled cluster theory for high spin, open shell reference wave function. *J. Chem. Phys.*, 99(7):5219, 1993.

[12] MOLPRO, a package of ab initio programs designed by H.-J. Werner and P. J. Knowles, version 2002.1, R. D. Amos, A. Bernhardsson, A. Berning, P. Celiani, D. L. Cooper, M. J. O. Deegan, A. J. Dobbyn, F. Eckert, C. Hampel, G. Hetzer, P. J. Knowles, T. Korona, R. Lindh, A. W. Lloyd, S. J. McNicholas, F. R. Manby, W. Meyer, M. E. Mura, A. Nicklass, P. Palmieri, R. Pitzer, G. Rauhut, M. Schütz, U. Schumann, H. Stoll, A. J. Stone, R. Tarroni, T. Thorsteinsson and H.-J. Werner.

[13] J. E. Rode, J. Klos, L. Rajchel, M. M. Szczesniak, G. Chalasinski, and A. A. Buchachenko. Interactions in open-shell clusters: Ab initio study of pre-reactive complex $O(^3P)$ + HCl. *J. Phys. Chem. A*, 109:11484, 2005.

[14] H.-J. Werner and P. J. Knowles. *J. Chem. Phys.*, 89:5803, 1988.

[15] P. J. Knowles and H.-J. Werner. *Chem. Phys. Lett.*, 145:514, 1988.